SCIENTIFIC REPORTS
nature research

OPEN

# Au-PDA@$SiO_2$ core-shell nanospheres decorated rGO modified electrode for electrochemical sensing of cefotaxime

M. Z. H. Khan[1*], M. Daizy[1], C. Tarafder[1] & X. Liu[2]

**In this work, we have successfully synthesized core-shell structured Au-PDA@$SiO_2$ nanospheres and decorated on reduced graphene oxide (rGO) modified glassy carbon electrode for the electrochemical detection of cefotaxime. The one-pot hydrothermal method was used to synthesis core-shell nanostructures by loading Au nanoparticles on polydopamine (PDA) coated $SiO_2$ nanospheres. The as-prepared Au-PDA@$SiO_2$ nanospheres were used to fabricate electrochemically reduced graphene oxide (rGO) modified glassy carbon electrode (Au-PDA@$SiO_2$/rGO/GCE) for electrochemical determination of cefotaxime. Scanning electron microscopy, powder x-ray diffraction, transmission electron microscopy, and Fourier-transform infrared spectroscopy were used to confirm the structure and morphology of the as-prepared nanospheres. Cyclic voltammetry (CV) and electrochemical impedance spectroscopy (EIS) were performed for electrochemical characterizations different modified electrodes. It was revealed that the nanocomposite modified electrodes exhibited excellent electrochemical performances for electrooxidation of target analytes and could achieve ultra-sensitive detections. A linear relationship was observed between peak currents and concentrations in the ranges of $1.0 \times 10^{-9}$ to $5.0 \times 10^{-8}$ M ($R^2 = 0.9877$), and $1.0 \times 10^{-7}$ to $5.0 \times 10^{-6}$ M ($R^2 = 0.9821$) for cefotaxime with a detection limit (S/N = 3) of $1.0 \times 10^{-10}$ M. It can be deduced that the proposed sensor is suitable for the sensitive detection of cefotaxime in pharmaceutical samples.**

Cefotaxime (CEF) belongs to the class of beta-lactam third generation cephalosporin antibiotic and own a broad spectrum of activity against both Gram positive and negative bacteria[1]. This semisynthetic antibiotic widely used to treat urinary tract infections, gonorrhea, pneumonia and pelvic inflammatory diseases[2]. Because of its crucial role in numerous pharmaceutical and pathological processes, it is essential to develop selective and sensitive detection and quantification of CEF. To date, several analytical methods have been reported for detection of CEF including chromatography[3], spectrophotometry[4], fluorescence[5], electrochemistry[1,2] etc. However, most of the analytical methods are costly, time consuming and need tedious pretreatment. On the other hand, electrochemical detection has been found more attractive due to their simplicity, higher sensitivity, low cost and selectivity over conventional methods.

Recently, graphene and reduced graphene oxide have attracted significant interest worldwide due to its extraordinary electrochemical properties, high surface area and high charge-carrier mobility[6–8]. Reduced graphene oxide was reported to provide an effective sensing platform for selective detection of bio-entities due to their tunable functionalities on their basal planes[9–12]. On the other hand, Silica nanoparticles based materials with tunable pore structures attracted significant attention in various electrochemical sensors[13]. Several works have been reported on polymer coated $SiO_2$ nano-spheres[14–17]. Among them, dopamine has attracted considerable attention due to its spontaneous oxidative polymerization to form polydopamine (PDA)[18–20]. PDA has been exploited as an adhesion layer to immobilize self-assembled monolayer, metal films[21], biological molecules[22], etc.

[1]Department of Chemical Engineering, Jashore University of Science and Technology, Jashore, 7408, Bangladesh. [2]College of Chemistry and Chemical Engineering, Henan University, Kaifeng, 475004, China. *email: zaved.khan@just.edu.bd

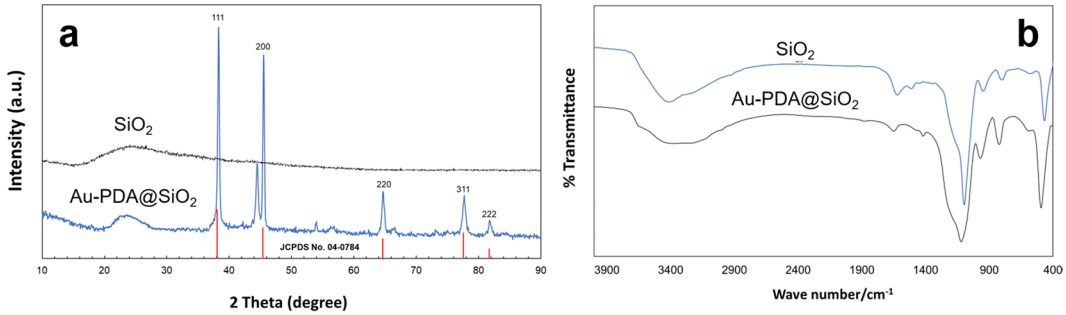


**Figure 1.** XRD pattern (**a**) and FTIR spectra (**b**) of $SiO_2$ and Au-PDA@$SiO_2$ nanocomposite.

to form biosensors[23–27]. Moreover, gold nanoparticles (AuNPs) have high surface reaction activity, strong adsorption ability, and good electrical properties. The incorporation of AuNPs was reported to enhance the sensitivity and selectivity of modified electrode platform[28].

In this work, we present a simple one-step controllable synthesis of core-shell structured Au-PDA@$SiO_2$ nanospheres and decorated on rGO modified glassy carbon electrode for the electrochemical detection of cefotaxime. The morphology and electrochemical properties of the prepared nano-sphere was investigated. Moreover, the real sample was analyzed to study the potential application of the modified electrode.

## Materials and Method

**Materials.** Tetraethylorthosilicate (TEOS), tetrachloroaurate ($HAuCl_4$), trihydrate ethanol and ammonium hydroxide ($NH_3.H_2O$, 25–28%) were purchased from Aladdin Reagent, Shanghai. Modified Hummers' method was used to produce graphene nanosheet from natural graphite powder and described in our previous paper[8]. Other chemicals were of analytical grade and used without further purification.

**Preparation on AuNPs colloidal solution.** Typically, 212 ml of DI water was vigorously stirred under reflux and 25 ml of 2.54 mM $HAuCl_4$ solution was added. The resultant solution was stirred until the boiling point achieved. Then, 12.5 ml of 10 mg/$ml^{-1}$ sodium citrate solution was added and the system was refluxed for 30 min, cooled at room temperature and kept in refrigerator at 4 °C.

**Synthesis of Au-polydopamine@$SiO_2$ core-shell nanospheres.** StÖber method was used to synthesis $SiO_2$ particles using tetraethylorthosilicate (10.8 ml) and ammonium hydroxide (17.0 ml). Later, the as-synthesized $SiO_2$ was dispersed in the buffer (Tris; 8.5 pH at 25 °C) and sonicated for 30 min. Then, 2 mg/ml dopamine hydrochloride was added in the solution with continuous stirring at 250 rpm for 6 h. Finally, pre-prepared AuNPs solution (0.5 mM) was added in the mixture during stirring and continued for 4 h. After completion of reaction, the mixture was centrifuged and washed several times to remove unattached AuNPs from PDA@$SiO_2$ surface.

***Preparation of* Au-PDA@$SiO_2$/rGO/GCE *electrode*.** Before modification, the bare GCE electrode was polished with 0.05 μ m alumina slurry. Later, the polished electrode was washed stepwise in ultrasonic bath with nitric acid (1:1), ethanol, and deionized water respectively. Finally, the cleaned electrode was rinsed with ultra-pure water and dried on air. The rGO was electrodeposited on GCE electrode through cyclic voltammetries between −1.3 and 0.7 V vs. Ag/AgCl for 15 cycles with a scan rate of 50 $mVs^{-1}$. After electrodeposition of rGO on GCE, the rGO/GCE electrode was washed with ultrapure water and air dried. On the other hand, 5 mg of Au-PDA@$SiO_2$ nanocomposite was dispersed in 1 ml of ethanol and dropwise cast (20 μl) on the pretreated rGO/GCE electrode surface. The modified electrode was named as Au-PDA@$SiO_2$/rGO/GCE modified electrode and used for electrochemical studies.

**Apparatus.** Corrtest electrochemical workstation (CS-300, Wuhan, China) was used for all electrochemical measurements. Surface morphology measurements were done using scanning electron microscopy (SEM) (Hitachi S-3000H, Japan), transmission electron microscope (TEM) (JEOL JEM-2100 model), and powder X-ray diffraction (XRD) (Bruker D8 Advance, Germany). Nitrogen ($N_2$) atmosphere and 25 °C temperature were maintained during electrochemical measurements.

## Results and Discussion

**Characterization of Au-polydopamine@$SiO_2$ core-shell nanospheres.** The wide-angle XRD patterns give the chemical composition and the crystalline nature of the as-prepared nanoparticles as illustrated in Fig. 1a. A broad scattering maximum centered at 22.5° corresponding to amorphous silica as reported in previous literature[29]. The decreased intensity of $SiO_2$ nanoparticles confirms the PDA coating. From the XRD pattern of Au-polydopamine@$SiO_2$, the peaks at $2\theta = 38.07°$, 44.24°, 64.43°, and 77.35° were indexed to (111), (200), (220), and (311) sets of planes of the face centered cubic structure of AuNPs (with reference to JCPDS File no. 04–0784) as shown in Fig. 1a.

Figure 1b shows the FTIR spectra of $SiO_2$ and Au-PDA@$SiO_2$ nanosphere. For $SiO_2$, the broad peak observed at 3415 $cm^{-1}$ is assigned to O-H stretching in silica, whereas the peak at 1619 $cm^{-1}$ is for O-H scissor bending vibration. On the other hand, the sharp peaks observed at 1109 and 799 $cm^{-1}$, respectively can be assigned to O-H

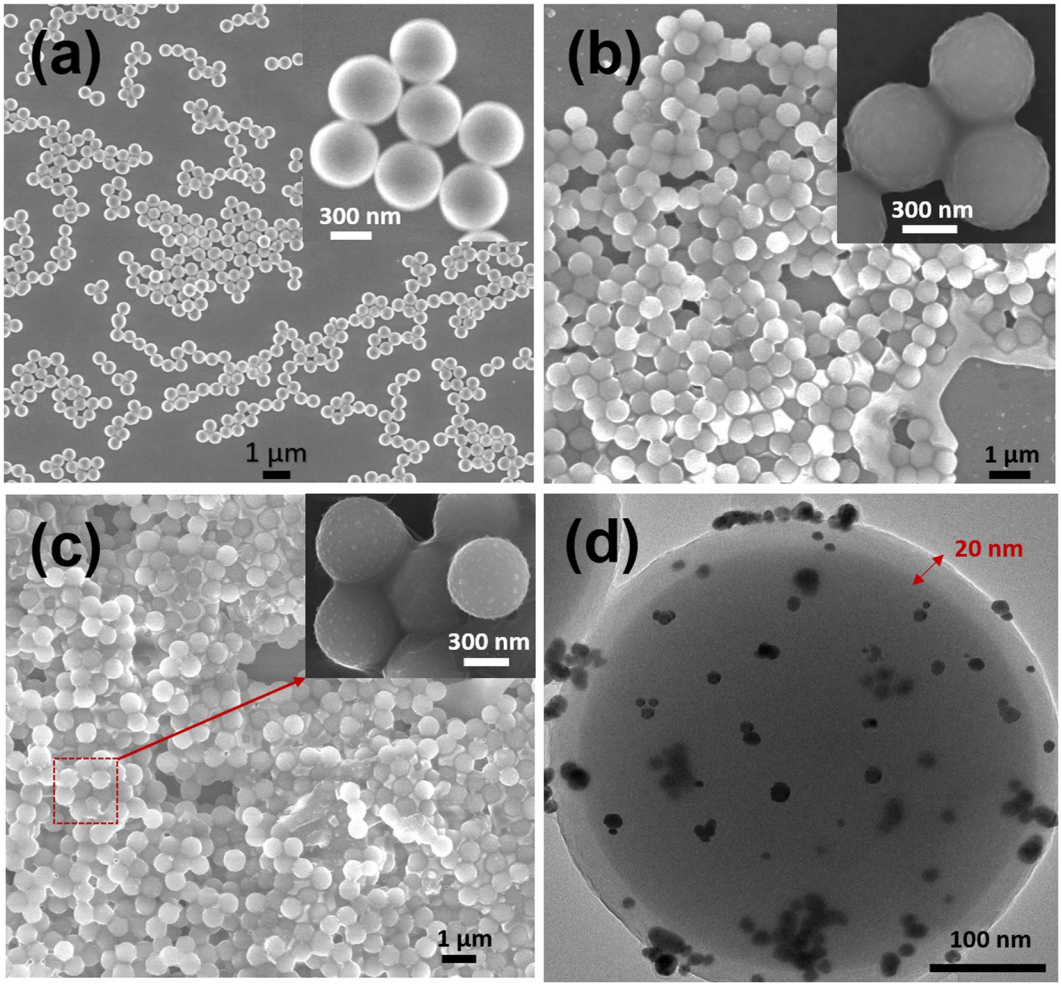


**Figure 2.** SEM images of (**a**) freshly prepared $SiO_2$ nanoparticles; (**b**) PDA@$SiO_2$ after coating with polydopamine; (**c**) AuNPs decorated on PDA@$SiO_2$ nanoparticles. The insets show the high magnification images. The high magnification TEM image of Au-polydopamine@$SiO_2$ core-shell nanospheres (**d**) clearly indicates the 20 nm layer of PDA coating and AuNPs decoration on $SiO_2$ particle.

ions as reported in literature[30]. After polydopamine coating on silica nanoparticle, indole aromatic ring vibrations were noticed at 1628 $cm^{-1}$ as reported by earlier researchers[28,31]. Moreover, the presence of PDA was confirmed by the peak at 3407 $cm^{-1}$.

SEM and TEM measurements were carried out to confirm the structural morphology of as-prepared nanocomposites. Figure 2a shows the SEM image of $SiO_2$. A well-defined spherical morphology was observed for $SiO_2$ particles with an average particle size of 400 nm. After the polymerization of dopamine on $SiO_2$, a thin layer appears on the surface of the $SiO_2$. It is difficult to distinguish the thin thickness shell of PDA due to lower contrast comparing with $SiO_2$. After polydopamine coating of $SiO_2$ particles, the PDA@$SiO_2$ has a size of 450 nm as shown in Fig. 2b. The AuNPs decorated on PDA@$SiO_2$ nanoparticles is shown in Fig. 2c. The presence of AuNPs on the surface of PDA@$SiO_2$ was confirmed by the clear bright spots from TEM images. Figure 2d also confirms the thickness of PDA shell (about 20 nm) on the surface of $SiO_2$ shell.

**Electrochemical characterization of the modified electrode.** Figure 3a represents CVs of the rGO electrodeposition on the GCE electrode (−1.3 and 0.7 V vs. Ag/AgCl; scan rate of 50 $mVs^{-1}$). The electrochemical performance of the bare and different modified electrodes was tested via CV in 5.0 mM $L^{-1}$ $Fe(CN)_6^{3-/4-}$ electrolytes as shown in Fig. 3b. Well defined redox peaks were observed for both bare and modified electrodes corresponds to $Fe(CN)_6^{3-/4-}$. A peak to peak separation ($\Delta E_p$) value of 211 mV was calculated for bare electrode that indicates slow electron-transfer kinetics at the surface. However, after rGO modification, the $\Delta E_p$ values were 85 mV suggesting larger electroactive surface. While after Au-PDA@$SiO_2$ deposition (Au-PDA@$SiO_2$/rGO/GCE), the $\Delta E_p$ value was 77 mV, which is larger than rGO/GCE but much higher than bare electrode. It can be deduced that due to synergetic amplification, conductive graphene sheets conjugated Au-PDA@$SiO_2$ nanosphere effectively facilitate electron transfer rate.

**Electrochemical behavior of CEF on modified electrodes.** Differential pulse voltammograms (DPV) method was used to study the electrochemical behavior of the modified electrode in the presence of different CEF

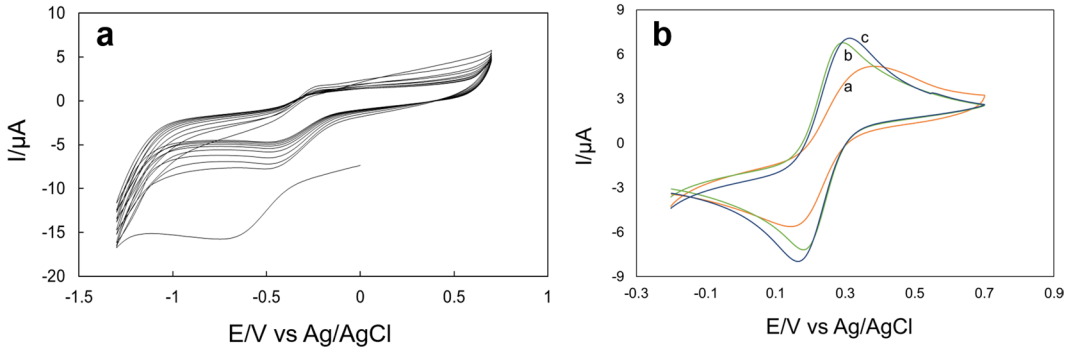


**Figure 3.** Cyclic voltammograms for (**a**) the electrochemical deposition/reduction of 0.5 mg ml$^{-1}$ GO nanosheets in 0.1 M PBS solution (pH 7.0) on GCE electrode at the scan rate of 50 mV/s for 15 cycles; (**b**) the bare and modified electrodes measured in 0.1 M L$^{-1}$ KCl including 5.0 mM L$^{-1}$ $Fe(CN)_6^{3-/4-}$: (**a**) bare GCE, (**b**) rGO/GCE, and (**c**) Au-PDA@$SiO_2$/rGO/GCE.

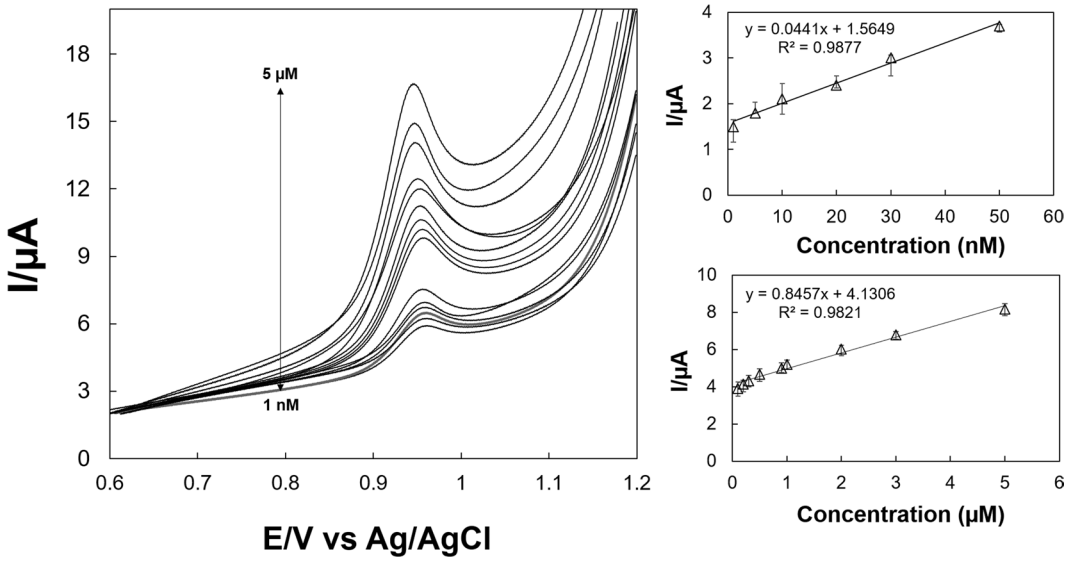


**Figure 4.** DPVs obtained for determination of CEF using Au-PDA@$SiO_2$/rGO/GCE modified electrode in pH 7.0 phosphate buffer at a scan rate of 50 mV s$^{-1}$ with a wide range of concentrations from $1.0 \times 10^{-9}$ M $- 5.0 \times 10^{-8}$ and $1.0 \times 10^{-7}$ M $- 5.0 \times 10^{-6}$ M. (**a**) All the graphs on the right side show the corresponding calibration curves for low (**b**) and high concentrations (**c**).

concentration and presented in Fig. 4. An accumulation time of 3 min in 0.1 M PBS (pH 7.0) was used during all experiments. It can be clearly noticed that the oxidative peak current ($I_{pa}$) increases with the concentration ($C$) of CEF as shown in DPV investigation (Fig. 4a). Two linear segments was observed from the calibration curve of CEF in the range from $1.0 \times 10^{-9}$ to $5.0 \times 10^{-8}$ M ($R^2 = 0.9877$), and $1.0 \times 10^{-7}$ to $5.0 \times 10^{-6}$ M ($R^2 = 0.9821$), with a LOD of (S/N = 3) of $1.0 \times 10^{-10}$ M (Fig. 4b,c). Table 1 represents the comparison of analytical findings of this study with several modified electrodes reported in literature.

**Reproducibility, stability and selectivity study.** To study the long-term stability and reproducibility of the proposed modified electrode, four freshly prepared Au-PDA@$SiO_2$/rGO/GCE electrodes were kept in refrigerator for 4 weeks at 4 °C temperature and the voltammograms were measured in PBS solution containing $1.0 \times 10^{-7}$ M CEF. Four replicate measurements show a standard deviation less than ±0.86 for DPV currents which confirms the reproductivity and stability of the proposed sensor. To study the selectivity of the proposed sensor, the effects of some common interferences on the determination of 1 μM CEF was tested. It was observed that 200-fold ascorbic acid, uric acid, and 100-fold glucose, L-glutamic acid did not influence the detection signal (<5%) of CEF measurement. These results indicate the good selectivity of the proposed method.

**Analysis of real samples.** In order to investigate the applicability of the proposed electrochemical sensor, recovery tests were performed for CEF in real urine samples. Prior to spiking different concentrations of CEF, healthy human urine samples were diluted 100 times using 0.1 M PBS (pH 7.0). The recovery results obtained from Table 2 demonstrates the possibility of the proposed sensor for real biological samples analysis.

| Electrode | Method | Linear range (μM) | LOD (μM) | Reference |
|---|---|---|---|---|
| AuNPs/Parg/CPE | Linear sweep voltammetry | 0.01–100 | 0.002 | [30] |
| Nano-Pd@ITO | Amperometry analysis | 0.1–0.7 | 0.06 | [31] |
| FeNP/GCE | Differential pulse voltammetry | 0.15–25 | 0.1 | [32] |
| MIP/GNWs@IL-PPNPs/COOH-rGO/GCE | Differential pulse voltammetry | 0.003–8.9 | 0.0001 | [1] |
| NaMM/ERGO/CPE | Differential pulse voltammetry | 0.0005–2.4 | 0.0001 | [2] |
| Au–PtNPs/MWCNT/GCE | Linear sweep voltammetry | 0.004–10.0 | 0.001 | [33] |
| Au-PDA@$SiO_2$/rGO/GCE | Differential pulse voltammetry | 0.001–5 | 0.0001 | This work |

**Table 1.** Comparison of the proposed method with other electrochemical methods recently reported for the determination CEF.

| Sample | Measurement | Added (M) | Detected (M) | Recovery (%) | RSD (%) |
|---|---|---|---|---|---|
| Urine 1 | 1 | $1.0 \times 10^{-8}$ | $1.01 \times 10^{-8}$ | 100.9 | 2.04 |
| | 2 | $5.0 \times 10^{-8}$ | $4.87 \times 10^{-8}$ | 97.40 | 1.80 |
| | 3 | $1.0 \times 10^{-6}$ | $0.98 \times 10^{-6}$ | 98.10 | 1.23 |
| Urine 2 | 1 | $1.0 \times 10^{-8}$ | $0.97 \times 10^{-8}$ | 97.21 | 1.92 |
| | 2 | $5.0 \times 10^{-8}$ | $5.11 \times 10^{-8}$ | 102.2 | 2.15 |
| | 3 | $1.0 \times 10^{-6}$ | $0.96 \times 10^{-6}$ | 96.40 | 1.02 |

**Table 2.** Determination of spiked CEF in real urine samples.

## Conclusion

The present work introduced an innovative Au-PDA@$SiO_2$/rGO/GCE modified electrode for the sensitive detection of CEF. The proposed sensor can measure target analytes at very low concentration with a detection limit of $1.0 \times 10^{-10}$ M. Comparing with other CEF sensors, the modified electrode shows wide linear range, long-term stability. Hence, this electrochemical sensor can be used successfully for the determination of CEF in pharmaceutical preparations.

Received: 12 October 2019; Accepted: 7 November 2019;
Published online: 13 December 2019

## References

1. Yang, G., Zhao, F. & Zeng, B. Electrochemical determination of cefotaxime based on a three-dimensional molecularly imprinted film sensor. *Biosens. Bioelectron.* **53**, 447–452 (2014).
2. Dehdashtian, S., Behbahani, M. & Noghrehabadi, A. Fabrication of a novel, sensitive and selective electrochemical sensor for antibiotic cefotaxime based on sodium montmorillonite nonoclay/electroreduced graphene oxide composite modified carbon paste electrode. *J. Electroanal. Chem.* **801**, 450–458 (2017).
3. Wang, Z., Song, Z. & Chen, D. Study on the binding behavior of bovine serum albumin with cephalosporin analogues by chemiluminescence method. *Talanta* **83**, 312–319 (2010).
4. El Walily, A. F. M., Gazy, A. A. K., Belal, S. F. & Khamis, E. F. Use of Cerium (IV) in the Spectrophotometric and Spectrofluorimetric Determinations of Penicillins and Cephalosporins in Their Pharmaceutical Preparations. *Spectrosc. Lett.* **33**, 931–948 (2000).
5. Blanchin, M. D., Rondot-Dudragne, M. L., Fabre, H. & Mandrou, B. Determination of cefotaxime, desacetylcefotaxime, cefmenoxime and ceftizoxime in biological samples by fluorescence detection after separation by thin-layer chromatography. *Analyst* **113**, 899–902 (1988).
6. Khan, M. Z. H. *et al.* Formation and Characterization of Copper Nanocube-Decorated Reduced Graphene Oxide Film. *J. Nanomater.* **2017** (2017).
7. Khan, M. Z. H. *et al.* Electrochemical detection of tyramine with ITO/APTES/ErGO electrode and its application in real sample analysis. *Biosens. Bioelectron.* **108**, 76–81 (2018).
8. Khan, M. Z. H., Shahed, S. M. F., Yuta, N. & Komeda, T. Deposition of an Ultraflat Graphene Oxide Nanosheet on Atomically Flat Substrates. *J. Electron. Mater.* **46** (2017).
9. Lv, S., Zhang, K., Zeng, Y. & Tang, D. Double Photosystems-Based z-Scheme' Photoelectrochemical Sensing Mode for Ultrasensitive Detection of Disease Biomarker Accompanying Three-Dimensional DNA Walker. *Anal. Chem.* **90**, 7086–7093 (2018).
10. Zeng, R., Luo, Z., Zhang, L. & Tang, D. Platinum Nanozyme-Catalyzed Gas Generation for Pressure-Based Bioassay Using Polyaniline Nanowires-Functionalized Graphene Oxide Framework. *Anal. Chem.* **90**, 12299–12306 (2018).
11. Zhou, Q., Lin, Y., Zhang, K., Li, M. & Tang, D. Reduced graphene oxide/BiFeO3 nanohybrids-based signal-on photoelectrochemical sensing system for prostate-specific antigen detection coupling with magnetic microfluidic device. *Biosens. Bioelectron.* **101**, 146–152 (2018).
12. Zhou, Q. *et al.* Reduced graphene oxide-functionalized FeOOH for signal-on photoelectrochemical sensing of prostate-specific antigen with bioresponsive controlled release system. *Biosens. Bioelectron.* **98**, 15–21 (2017).
13. Qiu, Z., Shu, J. & Tang, D. Bioresponsive Release System for Visual Fluorescence Detection of Carcinoembryonic Antigen from Mesoporous Silica Nanocontainers Mediated Optical Color on Quantum Dot-Enzyme-Impregnated Paper. *Anal. Chem.* **89**, 5152–5160 (2017).
14. Culbertson, J. Manuscript for. 1–8 (2009).
15. Palkovits, R. *et al.* Polymerization of w/o Microemulsions for the Preparation of Transparent $SiO_2$/PMMA Nanocomposites, https://doi.org/10.1021/LA050630K(2005).
16. Ohno, K., Morinaga, T., Koh, K., Tsujii, Y. & Fukuda, T. Synthesis of Monodisperse Silica Particles Coated with Well-Defined, High-Density Polymer Brushes by Surface-Initiated Atom Transfer Radical Polymerization, https://doi.org/10.1021/MA048011Q (2005).

17. Zhang, Y.-P., Lee, S.-H., Reddy, K. R., Gopalan, A. I. & Lee, K.-P. Synthesis and characterization of core-shell $SiO_2$ nanoparticles/poly(3-aminophenylboronic acid) composites. *J. Appl. Polym. Sci.* **104**, 2743–2750 (2007).
18. Seok, S., Choi, I., Lee, K. G., Choi, G. & Park, J. Dopamine – induced Pt and N – doped carbon @ silica hybrids as a high – performance membrane fuel cell anode catalyst of polymer. *RSC Adv.* **4**, supporting information (2014).
19. Liu, M. *et al.* A facile one-step method to synthesize $SiO_2$ @polydopamine core–shell nanospheres for shear thickening fluid. *RSC Adv.* **6**, 29279–29287 (2016).
20. Seok, S. *et al.* Dopamine-induced Pt and N-doped carbon@silica hybrids as high-performance anode catalysts for polymer electrolyte membrane fuel cells. *RSC Adv.* **4**, 42582–42584 (2014).
21. Ren, R., Cai, G., Yu, Z., Zeng, Y. & Tang, D. Metal-Polydopamine Framework: An Innovative Signal-Generation Tag for Colorimetric Immunoassay. *Anal. Chem.* **90**, 11099–11105 (2018).
22. Lin, Z. *et al. In situ* synthesis of fluorescent polydopamine nanoparticles coupled with enzyme-controlled dissolution of $MnO_2$ nanoflakes for a sensitive immunoassay of cancer biomarkers. *J. Mater. Chem. B* **5**, 8506–8513 (2017).
23. Xu, F. *et al.* Prepare poly-dopamine coated graphene@silver nanohybrid for improved surface enhanced Raman scattering detection of dyes. *Sensors Actuators, B Chem.* **243**, 609–616 (2017).
24. Dong, Y., Liu, T., Sun, S., Chang, X. & Guo, N. Preparation and characterization of SiO2/polydopamine/Ag nanocomposites with long-term antibacterial activity. *Ceram. Int.* **40**, 5605–5609 (2014).
25. Salazar, P., Martín, M. & González-Mora, J. L. Polydopamine-modified surfaces in biosensor applications. *Polym. Sci. Res. Adv. Prat. Appl. Educ. Asp.* **1**, 385–396 (2007).
26. Liu, R. *et al.* Dopamine as a carbon source: The controlled synthesis of hollow carbon spheres and yolk-structured carbon nanocomposites. *Angew. Chemie - Int. Ed.* **50**, 6799–6802 (2011).
27. Chen, J. *et al.* Catalase-imprinted $Fe_3O_4$/Fe@fibrous $SiO_2$/polydopamine nanoparticles: An integrated nanoplatform of magnetic targeting, magnetic resonance imaging, and dual-mode cancer therapy. *Nano Res.* **10**, 2351–2363 (2017).
28. Kar, P. *et al.* Facile synthesis of reduced graphene oxide–gold nanohybrid for potential use in industrial waste-water treatment. *Sci. Technol. Adv. Mater.* **17**, 375–386 (2016).
29. Zhang, Q. *et al.* Ag/$TiO_2$ and Ag/$SiO_2$ composite spheres: synthesis, characterization and antibacterial properties. *RSC Adv.* **3**, 9739 (2013).
30. Zhang, F. *et al.* Electrooxidation and determination of cefotaxime on Au nanoparticles/poly (L-arginine) modified carbon paste electrode. *J. Electroanal. Chem.* **698**, 25–30 (2013).
31. Gupta, S. & Prakash, R. Ninety Second Electrosynthesis of Palladium Nanocubes on ITO Surface and Its Application in Electrosensing of Cefotaxime. *Electroanalysis* **26**, 2337–2341 (2014).
32. Wang, M., Xu, X., Yang, J., Yang, X. & Tong, Z. Investigation of the electrocatalytic function of Fe3O4 nanoparticles and the application as cefotaxime sodium sensor. *Micro Nano Lett.* **6**, 284 (2011).
33. Shahrokhian, S. & Rastgar, S. Construction of an electrochemical sensor based on the electrodeposition of Au–Pt nanoparticles mixtures on multi-walled carbon n. *Analyst* **137**, 2706 (2012).

## Acknowledgements

We thank Prof. Yuta Nishina from University of Okayama, Japan for donating GO nanosheets. We also thank the Dept. of Glass and Ceramic Engineering, Bangladesh University of Engineering and Technology, Dhaka for microscopic measurement support.

## Author contributions

M.Z.H. Khan planned the work and wrote the manuscript. M. Daizy and C. Tarafder carried out experimental work. X. Liu supervised some part of this experiment.

## Competing interests

The authors declare no competing interests.

## Additional information

**Correspondence** and requests for materials should be addressed to M.Z.H.K.

**Reprints and permissions information** is available at www.nature.com/reprints.

**Publisher's note** Springer Nature remains neutral with regard to jurisdictional claims in published maps and institutional affiliations.